Controlled Nanopatterning of a Polymerized Ionic Liquid in a Strong Electric Field

Vera Bocharova, Alexander L. Agapov, Alexander Tselev, Liam Collins, Rajeev Kumar, Stefan Berdzinski, Veronika Strehmel, Alexander Kisliuk, Ivan I. Kravchenko, Bobby G. Sumpter, Alexei P. Sokolov, Sergei V. Kalinin, and Evgheni Strelcov*

Nanolithography has become a driving force in advancements of the modern day's electronics, allowing for miniaturization of devices and a steady increase of the calculation, power, and storage densities. Among various nanofabrication approaches, scanning probe techniques, including atomic force microscopy (AFM), are versatile tools for creating nanoscale patterns utilizing a range of physical stimuli such as force, heat, or electric field confined to the nanoscale. In this study, the potential of using the electric field localized at the apex of an AFM tip to induce and control changes in the mechanical properties of an ion containing polymer—a polymerized ionic liquid (PolyIL)—on a very localized scale is explored. In particular, it is demonstrated that by means of AFM, one can form topographical features on the surface of PolyIL-based thin films with a significantly lower electric potential and power consumption as compared to nonconductive polymer materials. Furthermore, by tuning the applied voltage and ambient air humidity, control over dimensions of the formed structures is reproducibly achieved.

1. Introduction

Nanofabrication is the basis for diverse areas of technology including electronics,[1,2] data storage,[3,4] sensors,[5,6] etc. Most conventional nanofabrication techniques have originated from various lithographical methods.[7–9] However, several critical limitations such as low resolution of conventional photolithography and high costs of e-beam and focused ion-beam lithographies are inhibiting future application of these techniques. In order to maintain the current pace of device miniaturization, it is crucially important to push forward the advancement of new nanofabrication methods and to expand the processable materials base.

A perspective tool for creating nanoscale patterning and nanofabrication is based on scanning probe technology.[10–12] Several atomic force microscopy (AFM)-based techniques utilize different physical stimuli, such as mechanical force, heat, electric field, and so on, that enable fabrication of structural features at the nanoscale.[13–16] Compared to the conventional lithography methods, AFM-based techniques provide the ease to achieve nanoscale resolution due to localization of the physical stimuli at the apex of an AFM probe, low costs, and compatibility with ambient conditions.

Driven by considerable structural versatility and relative material softness, polymers have been extensively studied as materials for direct nanopatterning and writing with AFM.[15–20] Several AFM-assisted patterning techniques, such as mechanical nanolithography,[13,14] thermomechanical writing,[15] electrostatic lithography,[16–19] and dip-pen nanolithography[20,21] have been employed to test predominantly nonconductive polymers, such as poly(methyl methacrylate) (PMMA) and polystyrene (PS). The potential of ion-containing polymers, such as polyelectrolytes or polymerized

Dr. V. Bocharova, Dr. A. Kisliuk, Prof. A. P. Sokolov
Chemical Sciences Division
Oak Ridge National Laboratory
Oak Ridge, Tennessee 37831, USA
E-mail: bocharovav@ornl.gov
Dr. A. L. Agapov, Prof. A. P. Sokolov
Department of Chemistry
University of Tennessee
Knoxville, Tennessee 37996, USA
Dr. A. Tselev, Dr. R. Kumar, Dr. I. I. Kravchenko,
Dr. B. G. Sumpter, Dr. S. V. Kalinin, Dr. E. Strelcov
Center for Nanophase Materials Sciences
Oak Ridge National Laboratory
Oak Ridge, Tennessee 37831, USA
L. Collins
School of Physics
University College Dublin
Belfield, Dublin 4, Ireland
Dr. R. Kumar, Dr. B. G. Sumpter
Computer Science and Mathematics Division
Oak Ridge National Laboratory
Oak Ridge, Tennessee 37831, USA
S. Berdzinski, Prof. V. Strehmel
Department of Chemistry and Institute for Coatings
and Surface Chemistry
Hochschule Niederrhein University of Applied Sciences
Adlerstrasse 32
D-47798, Krefeld, Germany

DOI: 10.1002/adfm.201402852

ionic liquids (PolyILs) for nanopatterning applications, is yet to be recognized and explored.

Being a synthetic product of polymerization of ionic liquids (ILs), PolyILs combine multiple strengths and viscoelastic properties of polymers with the high conductivity of room temperature ILs. These properties make PolyILs attractive candidates for various technological applications from lithium batteries to field-effect transistors and solar cells.[22,23] In comparison to conventional polyelectrolytes, PolyILs have weakly interacting organic cations and anions. Columbic interactions in such systems are only on the order of several kT, which gives rise to intriguing engagements between ionic transport and mechanical properties.[24,25] However, PolyILs present a relatively new class of materials that has not been studied in detail thus far. Recently, we reported[25] that a strong electric field applied to an apex of an AFM tip induces softening of PolyILs at nearly zero relative humidity. By drawing a parallel between changes in different ionic materials induced by a strong electric field[26–29] such as electrostriction in electrolyte solutions,[26] ionic dopant-controlled metal-insulator transistors,[27] an increase of ionic mobility in electrolytes[28] and surface conductivity of polyelectrolytes, e.g., DNA,[29] the origin of discovered phenomenon was proposed to stem from the ionic nature of PolyILs and the ability of electric field to dissociate ions and depress the glass transition temperature. Our previous work[25] focused on theoretical analysis of this phenomenon, while no detailed experimental studies or application of this phenomenon to nanopatterning has been presented or discussed. In contrast, this paper focuses on the experimental study of how the electric-field-induced transformation in PolyILs can be controlled and used for nanopatterning. In particular, we study how the size of topographical features is affected by the magnitude of the electric field and presence of humidity. An important advantage of studying PolyILs using an AFM setup is that the application of electrostatic potential directly to the AFM tip allows for localized control over ion transport. This can provide not only a method of polymer film patterning, but also a tool for precise analysis of structural and conductivity changes in the material. The PolyIL used for this study was poly(1-ethyl-3-vinylimidazolium) *bis*(trifluoromethylsulfonyl)imide. In this PolyIL, the anion is relatively small and mobile, while the cation is covalently attached to the polymer backbone and thus can be considered immobile in comparison to the anion (**Figure 1**). To the best of our knowledge, this is the first study that utilizes a polymeric material with weak Coulomb interaction to explore its behavior in a strong localized electric field for nanopatterning applications. The localization of a strong electric field, achieved by AFM, and the unique nature of the ion-containing polymers allow scaling down the size of the produced topographic features and establishing precise control over processes initiating their formation at the nanoscale.

2. Results and Discussion

We have used an AFM-based approach to generate patterns and to detect changes in the electrical and mechanical properties of PolyIL materials in a controlled humidity environment. A schematic of the experimental setup is shown in Figure 1. A single pulse (either rectangular or triangular) was applied to a conductive AFM tip in contact with a PolyIL film, whereas current was read-off of the bottom electrode with a simultaneous recording of the z-position (AFM height signal) of the tip. Changes in PolyIL properties were measured as a function of applied bias, relative humidity (RH), and time duration of the applied bias pulse. The main observation of the work is that if the tip bias voltage exceeded a certain threshold value, the voltage application resulted in softening of the PolyIL surface under the tip reflected in time-dependent changes of the tip z-position during application of a bias pulse. Apparently, the softening led to material compression/flow due to tip-induced pressure and formation of depression (holes) on the film surface. The produced holes can be directly visualized in topographic images acquired afterwards. Two qualitatively distinct regimes can be defined: "nanopatterning, with holes forming on the surface of a PolyIL" and "no nanopatterning", when hole formation could not be registered. The conditions for the hole formation and the hole dimensions were systematically studied using predefined spatial grids. In a typical measurement, the grid was 2×2 points; and a 2×5 or 10×10 grid was used to verify reproducibility of the pattern dimensions at fixed experimental conditions. Changes in the tip z-position and current–voltage (I–V) curves were averaged over all grid points. Importantly, application of negative biases led to poorly reproducible results; therefore, the grid pattern formation was studied in detail only with a positive bias applied to the AFM tip.

As discussed below, the exact value of the threshold voltage required for softening strongly depends on the environmental conditions. However, provided that voltage exceeded a threshold value, hole formation was observed at any humidity level and with any pulse shape. The RH plays a particularly important role in determination of the threshold voltage.

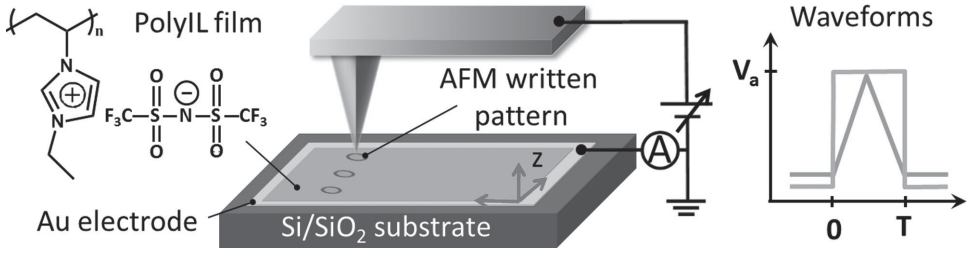

Figure 1. Schematic of the experimental setup used to pattern PolyIL thin film and to perform simultaneous measurements of the current and penetration depth of the AFM tip along the z-axis. Shapes of rectangular and triangular pulses used for polymer patterning are plotted schematically. V_a is the pulse amplitude, T is the pulse duration. Triangular pulses are symmetric.

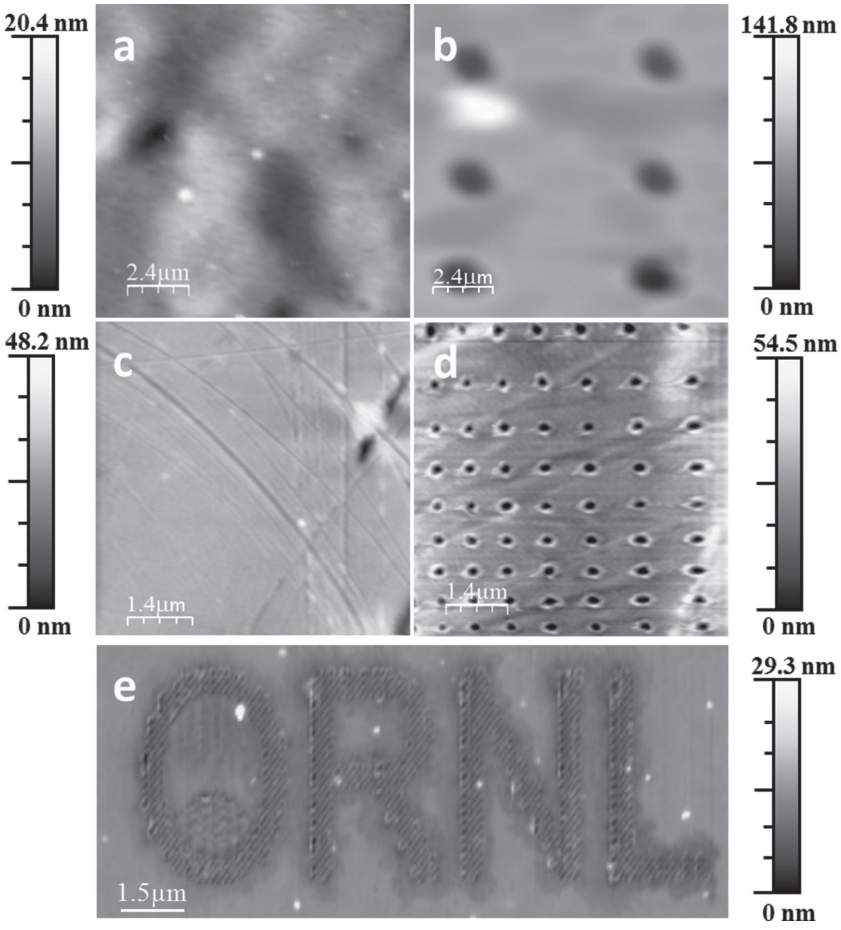

Figure 2. AFM topographic images of the 120-nm-thick PolyIL film after application of triangular voltage pulses with amplitudes of a) 10 V and b) 20 V at 0% RH, and with amplitudes of c) 2 V and d) 6 V at 40% RH. e) Example of patterning produced with pulses of +6 V amplitude applied to the tip for 250 ms at each point in the pattern. The distance between the points is ca. 100 nm.

The effect of RH on the threshold voltage for the case of triangular pulses is demonstrated in **Figure 2**. Specifically, at 0% RH, application of pulse amplitude above 10 V and pulse length above 8 s is required to generate holes (Figure 2a,b). In contrast, at 40% RH, softening starts above 2 V, whereas well-defined holes are formed at 6 V (Figure 2c,d). In turn, the dimensions of the holes are a complex function of RH as well as applied voltage. At 0% RH, the hole diameter is about 1 μm on average, (Figure 2b), whereas for 40% RH, it is approximately 300 nm (Figure 2d). The diameter of the holes indicates a tendency to decrease in response to the variation in applied voltage if humidity is held constant (Figure S1, Supporting Information). This finding suggests an interesting improvement of the experimental setup by use of ultrathin tips. Utilization of ultrathin tips could produce a more concentrated electric field and, as a result, a decrease in the diameter of the holes is expected. Interestingly, the hole diameters decrease with increasing humidity, while the depth shows the opposite trend. Namely, at 0% RH, a pulse amplitude of 20 V is required to form 25-nm-deep holes, whereas at 40% RH, formation of holes with the same depth occurs already at 6 V. Thus, control over the hole dimensions can be achieved via electric field and ambient air humidity.

Among the nanopatterns generated on different polymeric surfaces by means of AFM,[16–19] the PolyIL demonstrates a significantly reduced voltage required for surface patterning. For comparison, in case of nonconductive polymers the AFM tip-induced pattern formation was not observed at 0% RH, and a very high voltage (>20 V) was required to draw a structure at higher RH (≥40%).[19] Utilization of ion-containing materials provide a clear competitive advantage in patterning technology, as it allows for a decreased damage to the materials and reduced power consumption required for pattern fabrication. As an example, writing of a more complicated pattern in a 14 × 8 μm^2 area at ambient humidity using bias-induced softening is presented in Figure 2e.

The tip bias polarity has a strong effect on the softening of the PolyIL films, especially at lower humidity. For instance, at 0% RH, holes were not formed when the tip was negatively polarized. However, application of a positive tip bias above the threshold value resulted in formation of holes (**Figure 3**a). The maximal peak current in these experiments was ≈2.4 pA for a positive tip polarity and ≈0.7 pA for the reversed polarity (Figure 3b).

Application of voltage steps of different amplitudes at 0% RH revealed that the steady-state current has a nonlinear dependence on voltage (Figure 3c). Likewise, the deduced conductivity values follow a nonlinear trend (Figure 3c, inset). Experimental details of Figure 3c and their theoretical justification are provided in ref.[25] We exclude material degradation in a strong electric field as a possible explanation of nonlinearity because changes of PolyIL electrical conductivity induced by the electric field are in good agreement with the temperature-induced changes observed in electrical conductivity of an externally heated bulk PolyIL sample, as measured by broadband dielectric spectroscopy at a low applied voltage (<0.5V).[25] The detailed explanation is provided in ref.[25]

To explore the polymer softening further, we performed patterning experiments at different humidity levels. A systematic study of the tip penetration depth as a function of applied field and humidity is shown in the phase diagram of **Figure 4**a. Clearly, the formation of holes has a certain threshold voltage, which decreases with an increase in humidity (Figure 4b). The penetration depth of the tip also increases with increase in humidity and voltage (Figure 4a). Measurements in ten different spots (a 2 × 5 grid) performed for the selected humidity values of 6%, 36%, and 60% RH (Figure 4c) demonstrate that the hole size can be controlled by an electric field and humidity with a good precision. The *I*–*V* curves for the selected humidity values are shown in Figure 4d, where the inset illustrates the

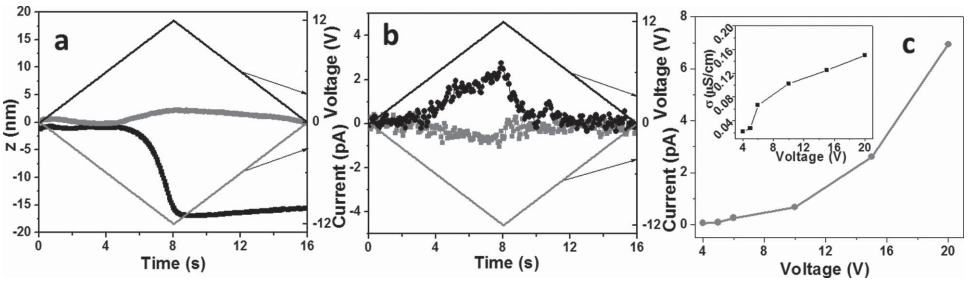

Figure 3. a) Tip *z*-position as a function of time observed during application of 12 V triangular pulses of positive (black) and negative (red) polarity at 0% RH and b) corresponding currents measured as a function of time. The bias waveforms are shown in panels (a) and (b) by solid lines. c) Current–voltage curves measured at 0% RH after application of voltage step. Inset shows the corresponding calculated conductivity.

tip *z*-position changes for the same humidity. A significant increase in current and hole depth is detected with increase in humidity. Furthermore, the current hysteresis is observed in the individual *I–V* curves. The hysteresis effect may likely occur due to the contribution from the changes in the film thickness upon softening and electrochemical processes in the sample. It should be mentioned that hole growth is terminated immediately after the potential is switched off. This is another advantage of using a localized electric field in achieving precise control over the size of the growing structures. However, extension of this patterning method to other ionic materials may be hindered without fundamental understanding of the nature of transformations occurring in the ionic material under strong electric fields.

To analyze possible mechanisms of the observed PolyIL softening, we first note that Joule heating is often employed to explain pattern formation with AFM tips in similar experiments with nonconductive polymers.[16–19] However, this mechanism cannot be the main reason for PolyIL softening in our experiments. Indeed, in case of thermally assisted patterning, a rather high power has to be generated before surface features begin to form. For example, in the case of PMMA a power of ≈3.2 μW (0.08 μA at 40 V at 40% RH) was necessary to generate a pattern.[19] In our patterning experiments at 0%, RH holes

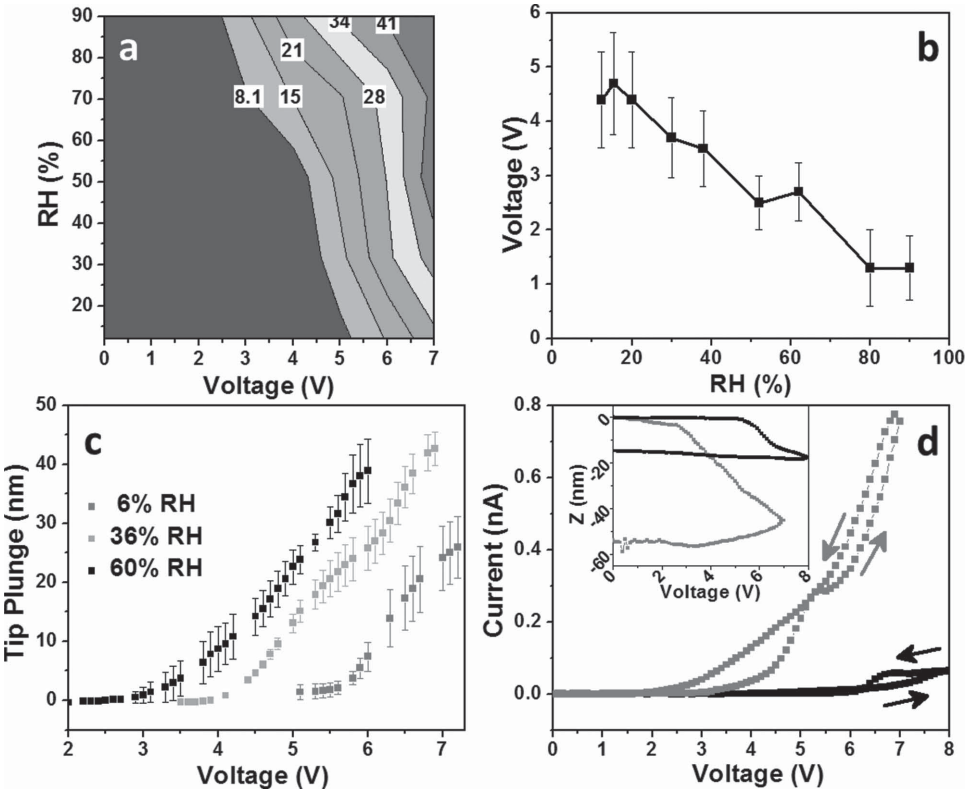

Figure 4. a) A map of the average tip penetration depth as a function of tip bias and ambient humidity. b) Threshold voltage as a function of RH. c) Curves representing cross-sections of the map in panel a) along the voltage axis at RH values of 6%, 36%, and 60%; d) Current–voltage curves measured for 11% RH (black) and 36% RH (red). The inset shows the corresponding change of the tip *z*-position. The direction of current flow is shown by arrows. The inset shows the corresponding tip *z*-position changes. The triangular pulses were applied to the PolyIL film of 120 nm.

were formed at a much lower power of 48 pW (2.4 pA at 20 V) and only with a positively biased tip. The difference between the experimental temperature (≈295 K) and the glass transition temperatures T_g of the PolyIL ($T_{g\ PolyIL}$ = 326 K) is three times smaller than that for PMMA ($T_{g\ PMMA}$ = 388 K), while the electric power in the case of PolyIL is more than 10 000 times smaller than the electric power generated during PMMA patterning. If the primary mechanism of pattern formation in PolyILs were Joule heating, then the threshold power would be on the same order of magnitude for both the PolyIL and PMMA, which is not the case. Furthermore, in our experiments with application of voltages of different polarity to the tip, the maximal electric power levels dissipated through the sample were comparable (Figure 3b), i.e., 48 pW (2.4 pA at 20 V) for the positive tip polarity and 14 pW (≈0.7 pA at 20 V) for the negative tip polarity. In the case of the heat-assisted pattern formation, similar patterns should have been formed for the same power, regardless of the tip polarity. In the control experiments with nonconductive PS (T_g = 379 K) under similar experimental conditions, formation of holes was not observed (Figure S2, Supporting Information). Additionally, numerical Finite Elements modeling using commercial software COMSOL was used to estimate the maximal temperature change caused by the Joule heat for our system. The details of this modeling are presented in ref.[25] The results showed a temperature raise by about 5 °C above the room temperature at maximum in the tip-surface junctions in our experiments. All this suggests that another mechanism different from Joule heating must be at play, a mechanism that is most likely linked to the ionic nature of the PolyIL sample.

Although the observed polymer softening in the presence of an electric field and humidity is apparently a multifaceted phenomenon, it is clear that several observations, including an asymmetric effect of the bias polarity, small currents, and nonlinearity of the *I*–*V* curves, are difficult to explain without implication of some mechanisms associated with ion-pair dissociation under an electric field in the PolyIL. In this regard, we note, that a high electric field of the order of 10^9 V m^{-1} is expected to appear near the tip-surface junction as a result of application of a few volts of bias to the tip due to a small radius of the tip apex. Multiple transport and material response mechanisms can be at play when strong electric fields appear under elevated humidity. Here, we consider that the observed effect is a superposition of multiple processes including water ionization, which happens at the field strength of ≈10^9 V m^{-1},[30] dissociation of the PolyIL, and Faradaic electrochemical processes in the PolyIL upon exceeding the voltage range of the electrochemical window.[31] The separation of contributions of the individual processes in such a complex system is a difficult task. Below we propose a scenario that may provide an explanation to the experimentally observed behavior of the PolyIL in the strong electric field at the tip apex.

We hypothesize that ions unbind at certain threshold voltage, which depends on humidity. Due to the sample nature, ion dissociation results in formation of mobile anions and significantly less mobile cations. In the absence of water, this dissociation requires a rather large activation energy of ≈3.5 eV,[32] which correlates well with our experimental observation of the high threshold voltage at 0% RH. At a high humidity, water molecules begin to form a solvation shell around bound ion pairs near the sample surface. This leads to a reduction of the activation energy for ion dissociation by providing a solvating environment characterized by a high dielectric constant. The dissociated anions then move towards the interface with the positively charged tip due to the attractive electrostatic forces and form an interfacial layer. The time required for the ions to electromigrate to the interface depends on the local viscosity and electric field. Indeed, we have observed the presence of a characteristic delay time between application of potential and actual changes of the mechanical properties. The delay time is well-resolved upon application of the step voltage to a thicker film (300 nm). The time delay depends on the relative humidity; for instance, at 11% RH and 10 V, it is ≈2.5 s (Figure S3a, Supporting Information), while it becomes undetectable at higher humidity (Figure S3b, Supporting Information). If we attribute this delay to the ion migration to the interface, then the roughly estimated mobility of 10^{-16}–10^{-17} m^2 V^{-1} s^{-1} (see Experimental Section for details) cannot be ascribed to migration of H^+ or OH^- ions with a mobility of 10^{-9} m^2 V^{-1} s^{-1}[33] in the polymer melts, but rather to migration of bulky anions of the PolyIL. Higher humidity leads not only to a better ion solvation, but also to a reduced local viscosity due to the general effect of plasticization;[34,35] so, ions diffuse faster in the PolyIL. As ions arrive at the interface, an uncompensated dense electrical charge starts to buildup. When the cumulative charge density reaches a critical value, it experiences an instability similar to electrohydrodynamic instabilities reported for nonconductive polymers[36,37] that stimulates softening of the polymer interface. Similar charge-induced softening in an electric field has been previously reported for the interface between the crystalline and superfluid ^{4}He,[38] where formation of ripplons was observed. In our case, this effect is not limited to the interface and can propagate inside the material since the concentration of ionic species in the polymer is very high. Also, the proposed scenario of softening explains why the tip has to be positively biased to induce hole formation: it has to be attractive for the mobile anions. When the tip is negatively charged, it will only attract the dissociated cationic chains of the PolyIL, which are too bulky and move too slowly to induce hole formation. Furthermore, the dynamics of hole growth after the softening under the tip can be qualitatively understood using theoretical analysis of the fastest growing mode[36,37] in the electrohydrodynamic instability. For example, the characteristic time scale[36,37] of the fastest growing mode is linearly proportional to the viscosity of the medium, and the assumption of reduced local viscosity with an increase in RH explains the disappearance of the lag time with an increase in relative humidity. Furthermore, approximating the diameter of the holes as the wavelength of the fastest growing mode, the observed decrease in the diameter of the holes with an increase in the applied voltage for a fixed humidity is in qualitative agreement with the predictions of the decrease in the wavelength with an increase in applied electric field.[37] However, the combined effect of humidity, dissociation of the ion-pairs, and possible Faradaic processes at higher applied voltage complicate the simple picture. The complete mechanism of softening and details of hydrodynamic analysis of hole formations are likely more complicated than suggested by our simple models and requires extensive

theoretical and experimental development to elucidate possible electrohydrodynamic instabilities in multicomponent system containing charged polymers and water.

3. Conclusion

In summary, we have demonstrated that by tuning the strength of electric field and the environmental conditions, one can form topographical features on the surface of a PolyIL in a reproducible manner with a good control over dimensions of the formed structures. The pattern formation for the ion-containing PolyIL occurs at a significantly lower strength of electric field and electric power as compared to nonconductive polymer materials. Although the mechanism of the pattern formation is complex and additional experiments are required to fully unveil contributions of the Faradaic processes as well as processes associated with ionization of water, the underlying PolyILs softening is undoubtedly dominated by the ion dissociation and electromigration in the polymer as opposed to Joule heating. These observations have promising implications for practical application of nanopatterning, where flexibility in pattern design and good control over the pattern lateral characteristics are necessary.

4. Experimental Section

Poly(1-ethyl-3-vinylimidazolium) *bis*(trifluoromethylsulfonyl)imide (Poly EtVImNTf2) PolyIL with a bulk T_g of 52.9 °C was dissolved in 2-butanone to a concentration of 6 mg mL^{-1}. Films of PolyILs were prepared by spin-coating a solution over a gold electrode predeposited on a Si/SiO_2 substrate. The thicknesses of the films were measured using profilometer and found to be 120 and 300 nm. The control measurements were performed on a 300-nm-thin film of nonconductive PS (PS, M_w = 100 kDa, T_g = 379 K) spin-coated from chloroform onto a gold electrode.

The change in electric current and the mechanical properties of the film as a function of applied voltage and humidity was monitored with conductive AFM (C-AFM). The two-electrode experimental setup is schematically illustrated in Figure 1 with the AFM tip acting as a top electrode and a gold surface being a bottom electrode. In the experiments, a rectangular or a triangular voltage pulse was applied to the PolyIL film via the AFM tip and current was collected from the bottom electrode. The duration of the triangular pulses can be estimated from the bias sweep rate of 0.4 s V^{-1}, and duration of rectangular pulses are shown on the corresponding figures. To limit current to ≈15 nA, an additional external resistance of 2 G Ω was connected in series with the sample. The pattern formation was observed at any applied bias waveform. The plunging of the tip (change of the tip *z*-position) was monitored electronically as a change in the voltage of the AFM controller applied to the z–piezo element needed to maintain a specified set point. In all experiments, the tip z–position feedback was switched on, so the force applied to the tip was constant during the experiment. Current and tip *z*-position were monitored in real time as a function of bias and ambient gas humidity. Current and z-position changes were measured at all locations of the selected grid over the sample surface and then averaged for certain bias values. The AFM was equipped with an environmental chamber allowing for fine regulation of the air relative humidity. For the measurements at 0% RH, samples were preconditioned at 100 °C in dry air flow to ensure evaporation of major part of the water layer from the sample surface prior to the measurements. Contact mode AFM was used to visualize changes in the film topography after application of voltage steps of different magnitudes. The spatial resolution of this method is limited by the tip radius, which was approximately 25 nm with the inner half conical angle of 23°.

The sample conductivity was calculated as $\sigma = \frac{I}{A}\frac{l}{V}$, where I is the current, V is the applied voltage, l is the sample thickness, and A is the tip-sample contact area. The change in the sample thickness as a result of tip plunge was taken into account in conductivity calculations. The first derivative was used to determine the threshold voltage from graphs of change in z as a function of applied voltage.

The mobility of the ions was calculated for the results obtained in Figure S3a (Supporting Information) as $\mu = \frac{\nu}{E}$, where ν is the drift velocity, E is the magnitude of the applied electric field. The drift velocity can be estimated from Figure S3a (Supporting Information): the delay time is 2.5 s. To estimate the distance ions migrated in this time, we note two relevant length scales: the distance that the tip plunged within 2.5 s is ≈20 nm, and distance that the tip plunged afterwards –≈200 nm. These distances reflect the thickness of the film layer that was affected by the electric field and underwent softening. Thus, the ion drift velocity is 8–80 nm s^{-1}. An estimate of the electric field strength beneath the tip was performed using COMSOL modeling and yielded (3–5) × 10^8 V m^{-1} (for tip bias of 10 V). Hence, the ion mobility is ≈(2–30) × 10^{-17} m^2 V s^{-1}.

The patterning example presented in Figure 2e was produced on a Cypher AFM (Asylum Research and Oxford Instruments Company, Santa Barbara). The custom lithography software written in Igor Pro (WaveMetrics, Inc.) was used to control tip position and bias application. At each point on the image, the tip was engaged to the surface and a short 250 ms pulse of a +6 V amplitude was applied to the tip. Then the tip was retracted and moved to the next position.

Supporting Information

Supporting Information is available from the Wiley Online Library or from the author.

Acknowledgements

V.B., R.K., and B.G.S. would like to acknowledge sponsorship by the Laboratory Directed Research and Development Program of Oak Ridge National Laboratory, managed by UT-Battelle, LLC, for the US Department of Energy. Work by A.K. and A.P.S. were supported by the US Department of Energy (DOE), Office of Science, Basic Energy Sciences (BES), and Materials Sciences and Engineering Division. A.L.A. thanks the NSF Polymer program (DMR-1104824). This research was conducted at the Center for Nanophase Materials Sciences, which is sponsored at Oak Ridge National Laboratory by the Scientific User Facilities Division, Office of Basic Energy Sciences, the US Department of Energy under user proposal No. CNMS2013–238. The authors would like to especially acknowledge Dr. Joshua R. Sangoro (University of Tennessee, USA) for providing a polymer sample for this study.

Received: August 19, 2014
Revised: November 6, 2014
Published online: December 17, 2014

[1] R. F. Pease, S. Y. Chou, *Proc. IEEE* **2008**, *96*, 248.
[2] H. M. Saavedra, T. J. Mullen, P. Zhang, D. C. Dewey, S. A. Claridge, P. S. Weiss, *Rep. Prog. Phys.* **2010**, *73*, 036501.
[3] B. D. Terris, T. Thomson, *J. Phys. D: Appl. Phys.* **2005**, *38*, R199.
[4] T. C. Chong, M. H. Hong, L. P. Shi, *Laser Photon. Rev* **2010**, *4*, 123.
[5] N. Verellen, P. Van Dorpe, C. Huang, K. Lodewijks, G. A. E. Vandenbosch, L. Lagae, V. V. Moshchalkov, *Nano Lett.* **2011**, *11*, 391.
[6] A. Kolmakov, M. Moskovits, *Annu. Rev. Mater. Res.* **2004**, *34*, 151.
[7] H. Klauk, D. J. Gundlach, M. Bonse, C. C. Kuo, T. N. Jackson, *Appl. Phys. Lett.* **2000**, *76*, 1692.

[8] J. Fujita, Y. Ohnishi, Y. Ochiai, S. Matsui, *Appl. Phys. Lett.* **1996**, *68*, 1297.
[9] L. Bach, I. P. Reithmaier, A. Forchel, J. L. Gentner, L. Goldstein, *Appl. Phys. Lett.* **2001**, *79*, 2324
[10] R. Garcia, A. W. Knoll, E. Riedo, *Nat. Nanotechnol.* **2014**, *9*, 577.
[11] C. F. Quate, *Surf. Sci.* **1997**, *386*, 259.
[12] E. S. Snow, P. M. Campbell, *Appl. Phys. Lett.* **1994**, *64*, 1932.
[13] B. Cappella, H. Sturm, *J. Appl. Phys.* **2002**, *91*, 506.
[14] Y. Sugimoto, M. Abe, S. Hirayama, N. Oyabu, O. Custance, S. Morita, *Nat. Mater.* **2005**, *4*, 156.
[15] W. P. King, T. W. Kenny, K. E. Goodson, G. Cross, M. Despont, U. Dürig, H. Rothuizen, G. K. Binnig, P. Vettiger, *Appl. Phys. Lett.* **2001**, *78*, 1300.
[16] S. F. Lyuksyutov, R. A. Vaia, P. B. Paramonov, S. Juhl, L. Waterhouse, R. M. Ralich, G. Sigalov, E. Sancaktar, *Nat. Mater.* **2003**, *2*, 468.
[17] S. F. Lyuksyutov, *Curr. Nanosci.* **2005**, *1*, 245.
[18] H. J. Chung, X. N. Xie, C. H. Sow, A. A. Bettiol, A. T. S. Wee, *Appl. Phys. Lett.* **2006**, *88*, 0231161300.
[19] X. N. Xie, H. J. Chung, C. H. Sow, A. A. Bettiol, A. T. S. Wee, *Adv. Mater.* **2005**, *17*, 1386.
[20] L. Huang, A. B. Braunschweig, W. Shim, L. Qin, J. K. Lim, S. J. Hurst, F. Huo, C. Xue, J.-W. Jang, C. A. Mirkin, *Small* **2010**, *10*, 1077.
[21] D. C. Coffey, D. S. Ginger, *J. Agric. Crop Sci.* **2005**, *127*, 4564.
[22] D. Mecerreyes, *Prog. Polymer Sci.* **2011**, *36*, 1629
[23] J. Y. Yuan, D. Mecerreyes, M. Antonietti, *Prog. Polymer Sci.* **2013**, *38*, 1009.
[24] J. R. Sangoro, C. Iacob, A. L. Agapov, Y. Wang, S. Berdzinski, H. Rexhausen, V. Strehmel, C. Friedrich, A. P. Sokolov, F. Kremer, *Soft Matter* **2014**, *10*, 3536
[25] R. Kumar, V. Bocharova, E. Strelcov, A. Tselev, I. I. Kravchenko, S. Berdzinski, V. Strehmel, O. S. Ovchinnikova, J. A. Minutolo, J. R. Sangoro, A. L. Agapov, A. P. Sokolov, S. V. Kalinin, B. G. Sumpter, *Nanoscale* **2014**, DOI: 10.1039/C4NR05491A.
[26] M. Yizhak, *Chem. Rev.* **2011**, *111*, 2761.
[27] C.-H. Yang, J. Seidel, S. Y. Kim, P. B. Rossen, P. Yu, M. Gajek, Y. H. Chu, L. W. Martin, M. B. Holcomb, Q. He, P. Maksymovych, N. Balke, S. V. Kalinin, A. P. Baddorf, S. R. Basu, M. L. Scullin, R. Ramesh, *Nat. Mater.* **2009**, *8*, 485.
[28] M. Wien, *Phys. Z.* **1928**, *29*, 751.
[29] a) C. Yamahata, D. Collard, T. Takekawa, M. Kumemura, G. Hashiguchi, H. Fujita, *Biophys. J.* **2008**, *94*, 63; b) T. Kleine-Ostmann, C. Jördens, K. Baaske, T. Weimann, M. Hrabé de Angelis, M. Koch, *Appl. Phys. Lett.* **2006**, *88*, 102102.
[30] T. D. Pinkerton, D. L. Scovell, A. L. Johnson, B. Xia, V. Medvedev, E. M. Stuve, *Langmuir* **1999**, *15*, 851.
[31] *Electrochemical Aspects of Ionic Liquids* (Ed: H. Ohno), Wiley, New York **2005**.
[32] B. Skinner, M. S. Loth, B. I. Shklovskii, *Phys. Rev. E* **2009**, *80*, 041925.
[33] A. R. Blythe, *Electrical Properties of Polymers, (in Cambridge Solid State Science Series)* Cambridge University Press, UK **1979**.
[34] W. G. Knauss, V. H. Kenner, *J. Appl. Phys.* **1980**, *51*, 5131.
[35] H. K. Nguyen, M. Labardi, M. Lucchesi, P. Rolla, D. Prevosto, *Macromolecules* **2013**, *46*, 555.
[36] T. P. Russell, J. Bau, in *Polymer, Liquids and Colloids in Electric Field, Vol. 2* (Eds: Y. Tsori, U. Steiner), (Series in Soft Condensed Matter), World Scientific, Singapore **2009**, Ch. 4.
[37] X.-F. Wu, Y. A. Dzenis, *J. Phys. D: Appl. Phys.* **2005**, *38*, 2848.
[38] D. Savignac, P. Leiderer, *Phys. Rev. Lett.* **1982**, *49*, 1869.